Contents lists available at ScienceDirect

Free Radical Biology and Medicine

Loss of C/EBPδ enhances IR-induced cell death by promoting oxidative stress and mitochondrial dysfunction

Sudip Banerjee [a], Nukhet Aykin-Burns [a], Kimberly J. Krager [a], Sumit K. Shah [a], Stepan B. Melnyk [b], Martin Hauer-Jensen [a,c], Snehalata A. Pawar [a,*]

[a] Division of Radiation Health, Department of Pharmaceutical Sciences, College of Pharmacy, University of Arkansas for Medical Sciences, Little Rock, AR 72205, United States
[b] Arkansas Children's Hospital Research Institute, Little Rock, AR 72205, United States
[c] Surgical Services, Central Arkansas Veterans Healthcare System, Little Rock, AR 72205, United States

ARTICLE INFO

ABSTRACT

Exposure of cells to ionizing radiation (IR) generates reactive oxygen species (ROS). This results in increased oxidative stress and DNA double strand breaks (DSBs) which are the two underlying mechanisms by which IR causes cell/tissue injury. Cells that are deficient or impaired in the cellular antioxidant response are susceptible to IR-induced apoptosis. The transcription factor CCAAT enhancer binding protein delta (Cebpd, C/EBPδ) has been implicated in the regulation of oxidative stress, DNA damage response, genomic stability and inflammation. We previously reported that Cebpd-deficient mice are sensitive to IR and display intestinal and hematopoietic injury, however the underlying mechanism is not known. In this study, we investigated whether an impaired ability to detoxify IR-induced ROS was the underlying cause of the increased radiosensitivity of Cebpd-deficient cells.

We found that Cebpd-knockout (KO) mouse embryonic fibroblasts (MEFs) expressed elevated levels of ROS, both at basal levels and after exposure to gamma radiation which correlated with increased apoptosis, and decreased clonogenic survival. Pre-treatment of wild type (WT) and KO MEFs with polyethylene glycol-conjugated Cu-Zn superoxide dismutase (PEG-SOD) and catalase (PEG-CAT) combination prior to irradiation showed a partial rescue of clonogenic survival, thus demonstrating a role for increased intracellular oxidants in promoting IR-induced cell death. Analysis of mitochondrial bioenergetics revealed that irradiated KO MEFs showed significant reductions in basal, adenosine triphosphate (ATP)-linked, maximal respiration and reserved respiratory capacity and decrease in intracellular ATP levels compared to WT MEFs indicating they display mitochondrial dysfunction. KO MEFs expressed significantly lower levels of the cellular antioxidant glutathione (GSH) and its precursor- cysteine as well as methionine. In addition to its antioxidant function, GSH plays an important role in detoxification of lipid peroxidation products such as 4-hydroxynonenal (4-HNE). The reduced GSH levels observed in KO MEFs correlated with elevated levels of 4-HNE protein adducts in irradiated KO MEFs compared to respective WT MEFs.

We further showed that pre-treatment with the GSH precursor, N-acetyl L-cysteine (NAC) prior to irradiation showed a significant reduction of IR-induced cell death and increases in GSH levels, which contributed to the overall increase in clonogenic survival of KO MEFs. In contrast, pre-treatment with the GSH synthesis inhibitor- buthionine sulfoximine (BSO) further reduced the clonogenic survival of irradiated KO MEFs.

This study demonstrates a novel role for C/EBPδ in protection from basal as well as IR-induced oxidative stress and mitochondrial dysfunction thus promoting post-radiation survival.

1. Introduction

Exposure to IR during cancer radiotherapy inevitably results in normal tissue toxicity to the rapidly renewing cell systems such as the hematopoietic tissues and the gastrointestinal tract mucosa [1–3]. The acute side-effects arise due to radiation-induced apoptotic and clonogenic cell death, and functional changes in various cellular compartments and microenvironments [1]. Although, several studies using cell lines and murine knockout models have demonstrated the role of genetics and genomics in toxic side-effects of radiotherapy, the molecular mechanism(s) of IR-induced injury in normal tissues remains unclear [2,3]. Knowledge of the underlying mechanisms is therefore critical for developing novel interventions to mitigate radiation-induced injury to the normal tissues [3].

IR exposure induces free radical generation and increased oxidative stress, which result in DSBs that are the primary causes of injury to cells and tissues [4–7]. It is known that exposure to IR induces a plethora of responses by cells to counteract oxidative stress, DNA damage response and inflammation by inducing the expression of antioxidants, DNA damage repair proteins and inflammatory and anti-inflammatory cytokines [7–11]. Cells have developed an antioxidant defense system to control the ROS [8,12,13]. If cells are deficient in the production of antioxidants to scavenge IR-induced oxidative stress and/or are impaired in the repair of IR-induced DSBs, they could be more sensitive to IR-induced apoptosis or become genetically unstable if they survive the initial IR insult [10,14]. Additionally, IR also affects the mitochondrial metabolism, which can lead to elevated levels of $O_2^{\bullet-}$ and thus perpetuate the damaging effects of IR in cells and tissues [14–17]. Most cellular ROS is generated in mitochondria, thus they play a key role in ROS-mediated apoptosis [15]. In the cells, ROS are mainly formed due to electron leakage naturally occurring in complex I and III of the mitochondrial electron transport chain [16]. Excessive and acute ROS accumulation triggers apoptotic pathway leading to cell death [17,18]. ROS, including superoxide ($O_2^{\bullet-}$) and hydrogen peroxide (H_2O_2) can cause oxidative damage via oxidation of DNA, proteins and lipids that may result in mitochondrial dysfunction [6,19]. The increase in ROS production leads to decreased ATP production, increased levels of protein carbonyls, and increased nitration of cellular proteins [20–22]. A balance between the production of ROS and the defensive capacity to produce antioxidants determines the ability of the cell to overcome oxidative damage [10,23].

The most abundant endogenous intracellular antioxidant present in the cells is the tripeptide L-γ-glutamyl-L-cysteinyl-glycine, GSH [24–27]. One of the major roles of GSH is to maintain the redox state that is critical for cellular activities [28,29]. Deficiency of GSH results in an increased pro-oxidizing shift and elevated oxidative stress [30,31]. The cellular biochemical machinery responsible for the metabolic production of free radicals and other reactive oxygen and nitrogen species derived from superoxide and nitric oxide could remain perturbed for minutes, hours, days and even years after exposure to IR [7].

The transcription factor C/EBPδ is a member of the basic leucine-zipper family of transcription factors that is implicated in the regulation of diverse biological processes in a cell-specific context such as acute phase response, proliferation, differentiation, growth arrest, apoptosis, hyperoxia, genomic stability, tumor suppression and self-renewal of stem cells [32–38]. The antioxidant enzyme SOD1 is a transcriptional target that is upregulated by C/EBPδ in cisplatin-treated human urothelioma cells and represents yet another important function for this protein [39].

Exposure to IR leads to increased oxidative stress, DNA-damage and inflammation, and although C/EBPδ is implicated in the regulation of these processes, how it regulates these processes in the context of IR is not clear [32,36,39–42]. We have recently reported that C/EBPδ-deficiency promotes increased radiation lethality primarily due to injury to the gastrointestinal and hematopoietic tissues, however the underlying mechanism has not been elucidated [43].

Here we investigated the role of C/EBPδ in modulating IR-induced oxidative stress and mitochondrial dysfunction to prevent cells from undergoing IR-induced cell death.

We report that C/EBPδ-deficiency is associated with increased oxidative stress and oxidative damage and results in an increased sensitivity of MEFs to IR-induced cell death. The increased oxidative stress and mitochondrial dysfunction and increased sensitivity of C/EBPδ-deficient cells is due to the reduced levels of the cellular antioxidant GSH and its precursor amino acid- cysteine as well as methionine.

2. Materials and methods

2.1. Ethics statement

This study was carried out in strict accordance with the recommendations in the Guide for the Care and Use of Laboratory Animals of the National Institutes of Health and approved by the Institutional Animal Care and Use Committee of the University of Arkansas for Medical Sciences (animal use protocol number: 3511).

2.1.1. Generation of primary mouse embryo fibroblasts (MEFs)

Primary MEFs were isolated from 13.5 day old *Cebpd*-KO and WT embryos as described previously [36] and grown in T-75 flasks in DMEM supplemented with 10% FBS, 2 mM glutamine, 0.5% penicillin-streptomycin, 50 μM β-mercaptoethanol, 1 mM sodium pyruvate. The cells were cultured at 37 °C in a humidified incubator with 5% CO_2 and 95% air. All studies were carried out on 2–3 pairs of early passage primary WT and KO MEFS (passage 3–7) in the presence of serum containing medium.

2.2. Reagents

NAC (Cat# A7250, St. Louis, MO) was prepared as 1 mM stock solutions with sodium bicarbonate and pH of 7.0. To prevent oxidation, NAC stocks were prepared fresh just before addition to the culture. BSO (cat# sc-200824, Santacruz Biotechnology, Dallas, TX), was dissolved in phosphate buffered saline (PBS) and prepared as a 10 mM stock solution.

2.3. Irradiation of MEFs

Irradiation (gamma-rays) of MEFs was performed in a Shepherd Mark I model 25 ^{137}Cs irradiator (J. L. Shepherd & Associates, San Fernando, CA). Dose uniformity was assessed by an independent company (Ashland Specialty Ingredients, Wilmington, DE) with radiographic film and alanine tablets. Alanine tablets were analyzed by the National Institute of Standards and Technology (Gaithersburg, MD) and demonstrated a dose rate of 1.14 Gy/min at 21 cm from the source. For each experiment the dose rate was corrected for decay.

2.3.1. Flow cytometry
2.3.1.1. Measurement of apoptosis

IR-induced cell death was measured with Annexin V FITC apoptosis detection kit (Cat # 556420, BD Biosciences, San Jose, CA, USA) and cleaved-caspase-3 expression. WT and KO MEFs (2×10^5 cells) were seeded per 60 mm dish in triplicates and 18 h

later exposed to 10 Gytt, and harvested at 0, 6 h and 24 h post-irradiation. The cells were detached with Accutase (Cat# AT104, Innovative Cell Technologies, Inc, San Diego, CA). Another set of dishes were treated with NAC (5 mM) for 2 h prior to IR exposure at 10 Gy. At 3 h post-irradiation, NAC containing media was replaced with a NAC-free medium and cells were harvested at 0 and 24 h post-irradiation and processed similarly for Annexin V staining as described above.

Staining of cleaved caspase-3 was used to further confirm late-apoptosis. 2×10^5 cells were seeded in 60 mm dishes and exposed to 10 Gy and harvested at 0 and 24 h post-irradiation. The cells were detached, washed with chilled PBS, stained with antibody specific for cleaved caspase-3 (Cat# 9644, Cell Signaling Technology, Danvers, MA, USA) and processed as per the manufacturer's instructions.

Cells stained for Annexin V as well as cleaved caspase-3 were analyzed immediately on a BD FACS Calibur 488 nm excitation wavelength with 530/30 nm (FL1) emission filter. For each analysis, 20,000 cells were assayed for fluorescence and the data were analyzed using FlowJo (FlowJo, LLC, Ashland, OR, USA) and results are expressed as mean fluorescence intensity of 20,000 cells $\pm$ standard error mean (S.E.M.).

2.3.1.2. Measurement of ROS

WT and KO MEFs were seeded at a density of 2×10^5 cells per 60 mm dish in triplicates and 18–20 h later exposed to 2 Gy . The cells were harvested 24 h later for measurement of ROS levels. At 24 h post-irradiation, cells were detached with 0.05% trypsin (Cat# 25300054, Thermo Fisher Scientific, Grand Island, NY), followed by a wash with PBS and were stained with 2 μM MitoSOX Red (Cat# M36008, Life technologies, Grand Island, NY, USA) at 37 °C for 15 min. Unirradiated WT and KO MEFs were processed similarly as irradiated groups. The stained cells were washed and suspended in 200 μl PBS and analyzed immediately on a BD FACS Calibur using 405 nm excitation wavelength with 585/642 nm (FL2) emission filter to detect ROS signal [44,45]. Results are expressed as mean fluorescence intensity of 20,000 cells $\pm$ S.E.M.

2.3.1.3. Clonogenic survival assay-dose curve

Clonogenic survival of MEFs was performed to compare the ability of cells to recover from radiation exposure and measure the differences in survival between WT and KO MEFs. Chinese hamster ovary (CHO) cells exposed to 35 Gy, were seeded at a density of 3×10^4 cells per well in six-well plates to serve as a feeder layer for the primary MEFs as has been described previously [46]. The irradiated CHO cells secrete growth factors into the medium which aid the growth of the primary MEFs.

WT and KO MEFs (2×10^5) cells were seeded in 60 mm petridishes, and 18 h later were exposed to irradiation doses of 0, 2, 4 and 8 Gy. The cells were re-seeded on the CHO feeder layers at low densities (50–300 cells/well) 3 h post-irradiation. Unirradiated WT and KO MEFs were treated similarly and seeded at various cell densities to measure the plating efficiency and used to calculate the percent survival as described previously [47]. By day 10–14 post-seeding, the CHO cells undergo cell death by mitotic catastrophe, while the MEFs form colonies. A negative control dish with no MEFs is included as a control and shows no colonies. At 2 weeks post-seeding, the colonies were fixed with chilled methanol (100%) for 30 min, followed by staining with Giemsa stain and were counted with a stereomicroscope. Colonies were defined as containing at least 50 cells. The plating efficiency and surviving fractions were calculated as described previously [47].

2.3.1.4. Clonogenic assay with antioxidant enzymes

PEG-SOD and PEG-CAT
(Sigma, St. Louis) were dissolved in sterile PBS at 5000 U per ml or 50,000 U per ml for stock solutions respectively. WT and KO MEFs were treated at a concentration of 50 U per ml for 2 h prior to irradiation at 2 Gy with PEG-SOD/PEG-CAT or in combination. PEG alone was used as a control. The cells were seeded on the irradiated CHO feeder layer and processed similarly as described above.

2.3.1.5. Clonogenic assay with NAC and BSO

For determining the effects of GSH levels on clonogenic survival, MEFs were treated with 5 mM NAC for 2 h prior to irradiation (2 Gy) and removed 3 h post-irradiation, when cells were re-seeded for the clonogenic assay in NAC-free medium. An aliquot of the treated cells was frozen for GSH measurements.

We also examined whether inhibition of GSH biosynthesis would further increase sensitivity of KO MEFs to IR. WT and KO MEFs (2×10^5) were seeded in 60mm dishes and 18h later treated with 10 μM BSO for 24 h prior to irradiation at 2 Gy. Cells were re-seeded 3 h post-irradiation in BSO-free medium on the irradiated CHO feeder layer and processed similarly as described above.

2.3.1.6. Immunoblotting

WT and KO MEFs (2×10^5) were seeded in 60 mm dishes and 18 h later exposed to 2 Gy. The cells were harvested and whole cell extracts were prepared at 0, 2 h, 4 h and 24 h post-irradiation. 50 μg protein was run on SDS-PAGE gels and immunoblotted. The blot was blocked with 5% milk in 10 mM Tris·HCl at pH7.5, 150mMNaCl and 0.05%Tween20 (1X TBST) probed with rabbit polyclonal serum against 4-HNE (1:10,000) in 1 X TBST. The blots were developed using peroxidase-conjugated anti-rabbit -secondary IgGs and visualized by ECL. Ponceau S staining of the blot served as a loading control for each sample per lane.

2.3.1.7. Mitochondrial cellular bioenergetics

We used the Seahorse Extracellular Flux 96 Analyzer (Agilent Biotechnologies, Santa Clara, CA, USA) to measure the oxygen consumption rate (OCR), an indicator of mitochondrial respiration in real-time in WT and KO MEFs. Briefly, 2×10^5 MEFs were seeded in 60 mm dishes and 18 h later exposed to 2 Gy. At 6 h post-irradiation, cells were trypsinized and 10^4 cells/well were seeded in Seahorse XF96 cell culture microplates and allowed to grow overnight at 37 °C. The cells were washed and subsequently changed to unbuffered seahorse assay medium at 24 h post-irradiation and the oxygen consumption rate (OCR) was measured using a 2 min mix, 4 min read cycling protocol as described previously [48]. The basal respiration, ATP-linked respiration, maximal respiration, reserved respiratory capacity, non-mitochondrial respiration and proton leak was calculated [49].

2.3.1.8. Measurement of ATP levels

WT and KO MEFs (8×10^5) were seeded in 100 mm dishes and 18 h later exposed to 2 Gy and cells were collected 24 h post-irradiation and flash frozen. Adenosine 5′-triphosphate (ATP) levels were measured using the ATP Bioluminescent Assay kit (Cat# FLAA, Sigma-Aldrich, St. Louis, MO) as per the manufacturer's instructions [50]. Standard curve for ATP was generated and total ATP levels were extrapolated and expressed as nmoles per cell.

2.3.1.9. Measurement of NADH, NAD, NADP, NADPH, GSH, GSSG, Methionine and Cysteine

WT and KO MEFs were seeded at a density of 8 x 10^5 cells per 100 mm dishes in triplicates and 18 h later were exposed to 2 Gy. The cell were harvested 24 h post-irradiation, snap-frozen in liquid nitrogen and stored at −80 °C until HPLC analysis. Nicotinamide adenine dinucleotide (NAD^+) and dihydronicotinamide adenine dinucleotide (NADH); nicotinamide adenine dinucleotide ($NADP^+$) and dihydronicotinamide adenine dinucleotide (NADPH)

were measured as described [51] utilizing a Dionex UltiMate 3000 HPLC-UV system (Dionex Inc., Sunnyvale, CA). C18 Gemini column (5 μm, 3 × 150 mm; Phenomenex, Torrance, CA) at 254 nm wavelength. Concentrations were calculated from peak areas of standard calibration curves using HPLC software. Results are expressed per mg protein using BCA Protein Assay Kit (Pierce Inc., Rockford, IL, USA).

For quantification of intracellular free GSH, glutathione disulfide (GSSG), methionine and cysteine, thawed cells were lysed by sonication in 112.5 μl ice-cold PBS followed by the addition of 37.5 μl ice-cold 10% meta-phosphoric acid. This mixture was incubated for 30 min on ice followed by centrifuging for 15 min at $18,000 \times g$ at 4 °C. The metabolites were eluted using a Shimadzu Solvent Delivery System (ESA model 580; ESA Inc., Chelmsford, MA) and a reverse-phase C18 column (3 μm, 4.6 × 150 mm; Shiseido Co., Tokyo, Japan). A 20 μl aliquot of cell extract was directly injected onto the column using an ESA Inc. Autosampler (model 507E), and the metabolites were quantified using a model 5200A Coulochem II and CoulArray electrochemical detection system (ESA) equipped with a dual analytical cell (model 5010), a 4-channel analytical cell (model 6210), and a guard cell (model 5020) as described previously [52].

2.3.1.10. Statistical analyses

Statistical analysis was performed using GraphPad Prism 7.0 (GraphPad Software, San Diego, California). Data were expressed as average ± standard error mean (S.E.M.) unless otherwise specified. One-way ANOVA with Tukey's post-analysis was used to study the differences among 3 or more means. $P < 0.05$ was considered statistically significant.

3. Results

3.1. Cebpd-deficiency increased IR-induced cell death in MEFs

We have shown that *Cebpd* plays an important role in the post-radiation survival of mice [43], so we first examined whether KO MEFs were also sensitive to IR exposure. Under basal conditions and at 6 h post-irradiation at 10 Gy, there were slightly more Annexin V positive KO MEFs than WT MEFs, but these differences were not significant. However, at 24 h post-irradiation, the number of Annexin V-positive KO MEFs was 1.8-fold higher than the respective WT MEFs (Fig. 1A).

We then examined the production of cleaved caspase-3, a marker of late apoptosis under basal conditions and 24 h
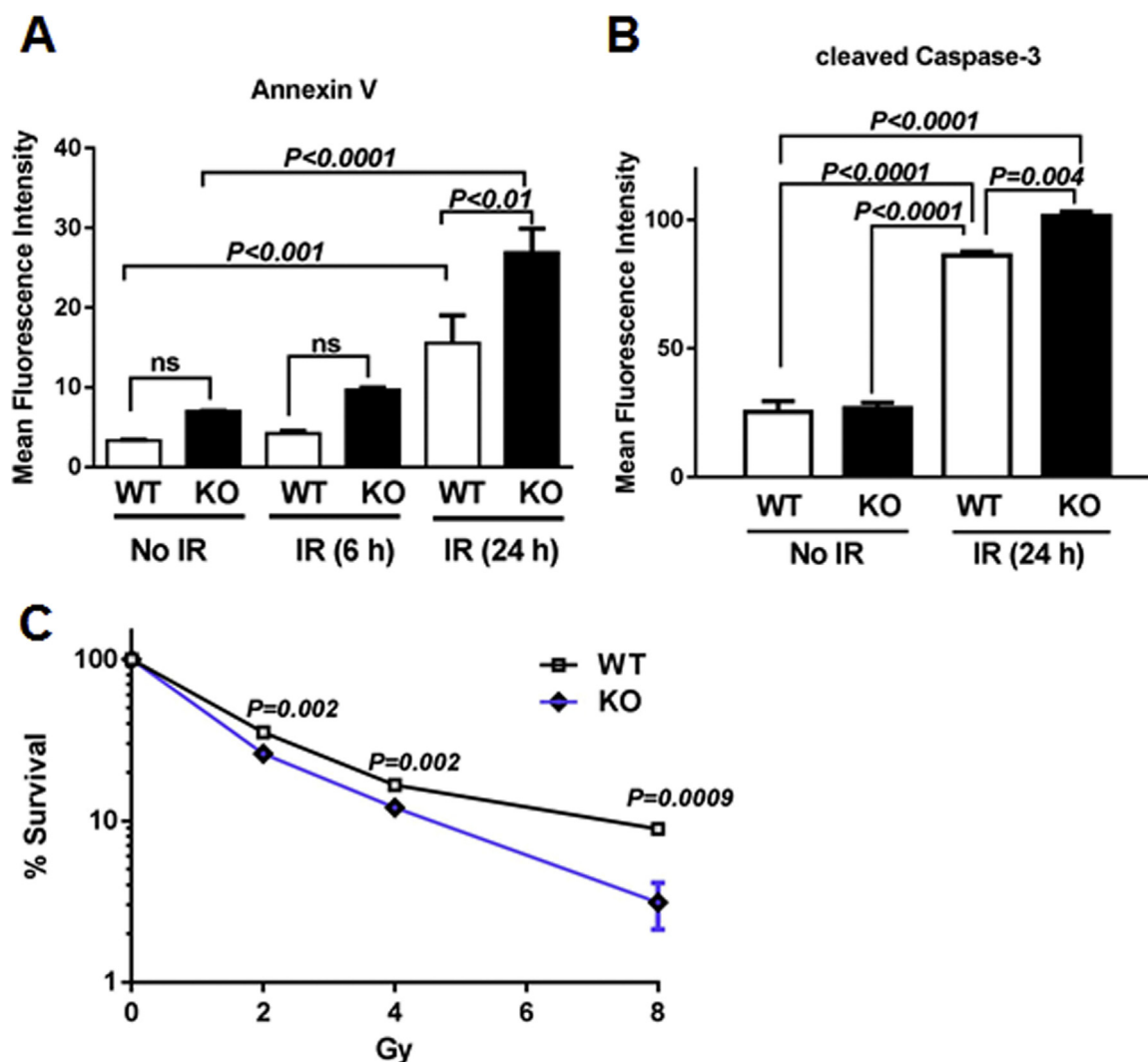

Fig. 1. *Cebpd*-KO MEFs show increased apoptosis and decreased clonogenic survival after exposure to IR. WT and KO MEFs were seeded in triplicates and harvested at 0, 6 h and 24 h post-irradiation (10 Gy), for (A) Annexin V staining and (B) cleaved caspase-3 staining and analyzed by flow cytometry. Data are represented as mean fluorescence intensity ± SEM. (C) KO and WT MEFs were exposed to 0–8 Gy and re-seeded 3 h later in triplicates. Colonies were scored 2 weeks later after staining with Giemsa. The data are presented as an average of 3 dishes seeded per treatment group, ns-not significant.

post-10 Gy exposure. Under basal conditions, there were no significant changes in cleaved caspase-3 expression between WT and KO MEFs. However 24 h post-irradiation, there was a robust increase in the amount of cleaved caspase-3 positive cells in both WT (3.4-fold) and KO MEFs (3.8-fold) compared to unirradiated WT controls. Irradiated KO MEFs expressed about 1.2-fold higher cleaved caspase-3 positive cells compared with irradiated WT MEFs (Fig. 1B), thus confirming that these cells undergo IR-induced apoptosis.
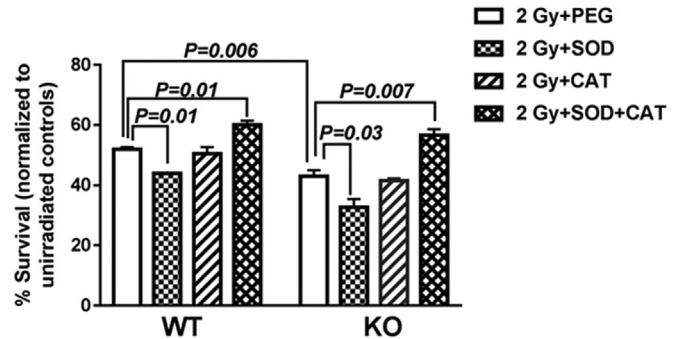
Next, we utilized the clonogenic survival assay to determine the effect of increasing doses of radiation on recovery and survival of MEFs and whether C/EBPδ-deficiency resulted in a differential response. While there were no significant differences in the number of clones in the unirradiated group between the genotypes (*data not shown*), KO MEFs showed a remarkable dose-dependent decline in survival of clones with increasing doses of IR compared to respective WT MEFs (Fig. 1C). These results suggest that C/EBPδ is essential to promote post-radiation survival which may be dependent upon its role in the modulation of radiation-induced oxidative stress.

3.2. Cebpd-deficiency promotes increased levels of intracellular oxidants

In order to investigate whether the increased sensitivity of KO MEFs to IR was due to the increased levels of oxidants, we first compared the cellular ROS levels at steady state levels and 24 h post-2 Gy exposure in WT and KO MEFs. WT and KO MEFs were stained with MitoSOX at 0 and 24 h post-2 Gy exposure and MitoSOX oxidation was analyzed by flow cytometry. Irradiated WT MEFs did not show a significant increase in MitoSOX oxidation compared to unirradiated WT MEFs (Fig. 2A-B). In contrast, we found that the basal levels of MitoSOX oxidation in KO MEFs were 1.8-fold higher compared to that of WT MEFs. At 24 h post-irradiation, KO MEFs showed 2.2-fold higher levels of MitoSOX oxidation compared to the WT MEFs (Fig. 2A-B). Although the basal levels of ROS are elevated in the KO MEFs, they are able to proliferate normally. However in response to an external stressor such as IR, KO MEFs show increased production of IR-induced ROS levels suggestive of an impaired oxidant/anti-oxidant balance as well as impaired mitochondrial function, since mitochondria are a
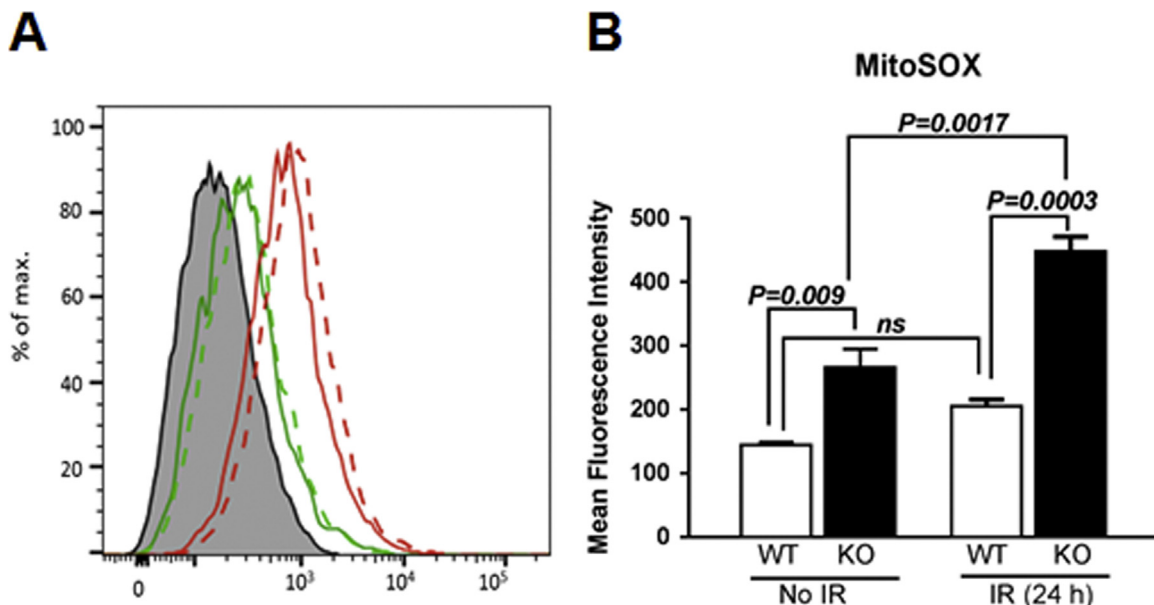
Fig. 3. PEG-SOD+CAT treatment prior to irradiation show a slight increase in post-radiation clonogenic survival of WT and KO MEFs. WT and KO MEFs were treated with PEG alone, PEG-SOD, PEG-CAT and or PEG-SOD+CAT for 2 h prior to irradiation at 2 Gy. The cells were re-seeded 3 h post-irradiation in triplicates and colonies were counted two weeks later and normalized to respective unirradiated dishes. The data are presented as an average of 2 biological relicates ± S.E.M. of 3 dishes seeded per treatment group.

significant source of superoxide.

3.3. Pre-treatment with exogenous antioxidant enzymes increased post-radiation clonogenic survival of Cebpd-KO MEFs

Based on our MitoSOX data, we hypothesized that KO MEFs are more radiosensitive than WT MEFs because they are unable to modulate the IR-induced oxidative stress. To determine whether impaired oxidative stress modulation is the underlying cause of the increased radiosensitivity of KO MEFs, we examined the clonogenic survival of WT and KO MEFs in the presence of exogenously added antioxidant enzymes. Since IR is known to induce $O_2^{\bullet-}$ and H_2O_2, we utilized superoxide dismutase which dismutates $O_2^{\bullet-}$ to form H_2O_2 and catalase that catalyzes the breakdown of H_2O_2 to water and molecular oxygen. WT and KO MEFs were pre-treated with PEG-SOD or PEG-CAT alone or in combination prior to irradiation.

Interestingly, pre-treatment of MEFs with PEG-SOD prior to IR exposure led to a 0.82-fold reduction in survival of WT MEFs and a 0.63-fold reduction in clonogenic survival of KO MEFs compared with PEG alone. These results suggest that the IR-induced $O_2^{\bullet-}$

Fig. 2. *Cebpd*-KO MEFs express increased ROS levels. WT and KO MEFs were exposed to 0 and 2 Gy, and 24 h later stained with MitoSOX and analyzed by flow cytometry. The data is presented as an average of 3 dishes seeded per treatment group and represented as mean fluorescence intensity ± S.E.M.
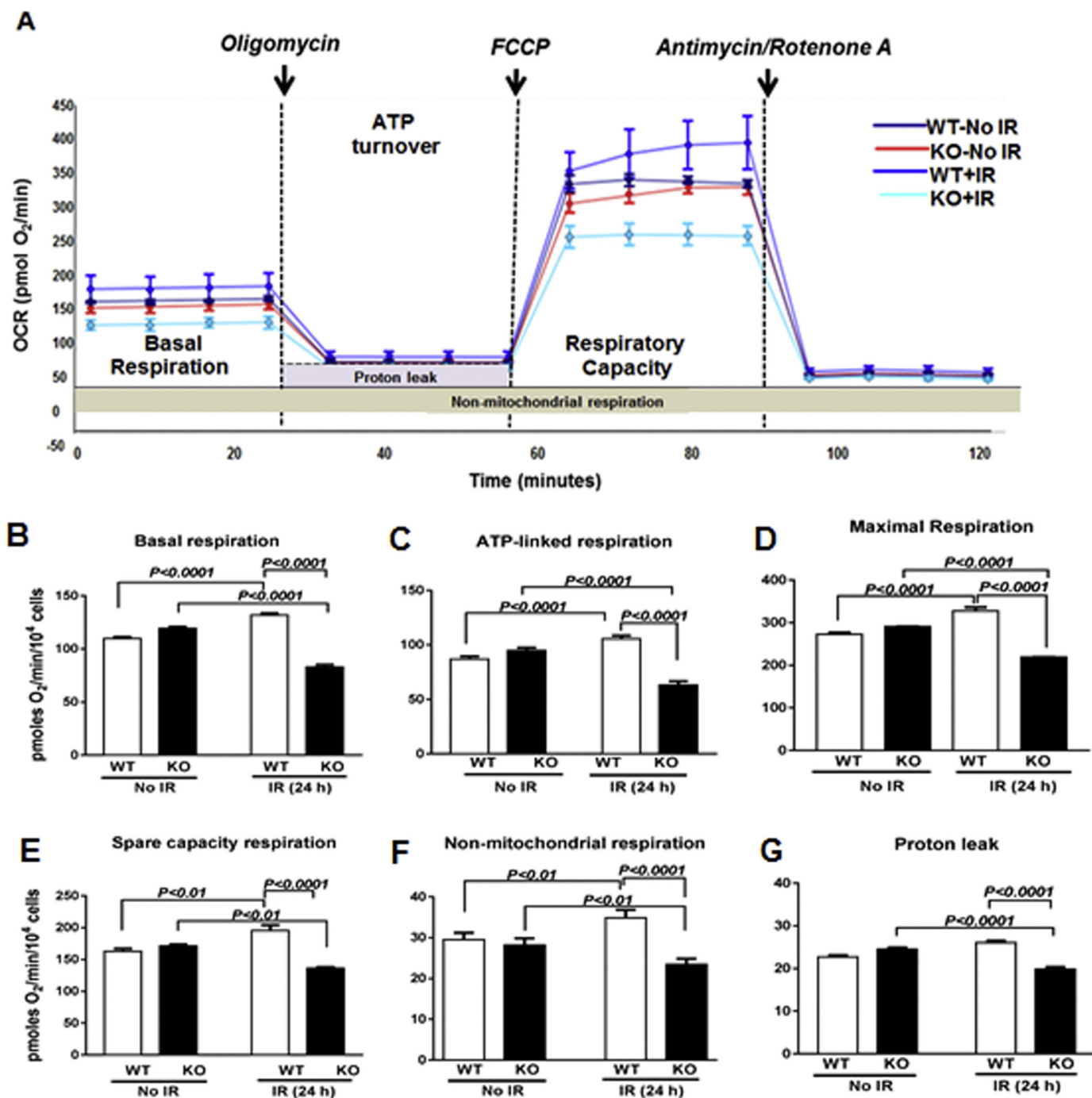
Fig. 4. *Cebpd*-KO MEFs showed decrease in mitochondrial bioenergetics after IR exposure. (A) Mitochondrial bioenergetics profiles were measured by seahorse XF-analyzer in sham and irradiated WT and KO MEFs. The arrows indicate the time of addition of mitochondrial inhibitors: oligomycin (1 μm), FCCP (5 μm) or rotenone and antimycin A (10 μm). (B) basal respiration; (*C*) ATP-dependent respiration; (D) Maximal respiration rate; (E) Reserved respiratory capacity; (F) non-mitochondrial respiration and (G) proton leakage between WT and KO MEFs. The data are presented as average ± S.E.M. of n=4–8 wells per treatment group.

species are converted to H_2O_2. The endogenous catalase in the irradiated WT and KO MEFs is not effective in catalyzing the increased H_2O_2 levels and thus leads to reduced clonogenic survival when compared to respective PEG-alone controls.

In contrast pre-treatment with PEG-CAT alone prior to IR exposure did not show any significant change in clonogenic survival in both irradiated WT and KO MEFs compared to their respective PEG alone groups. These results suggest that the IR-induced cell death that occurs in both WT and KO MEFs is perhaps due to the increased IR-induced $O_2^{\bullet-}$ and that the endogenous Cu-Zn SOD and Mn-SOD are not efficient in dismutation of $O_2^{\bullet-}$ or may be inactivated by IR-induced oxidative stress.

However PEG-SOD+CAT combination treatment prior to IR exposure showed a modest but significant increase in clonogenic survival of both WT and KO MEFs compared to respective PEG alone groups (Fig. 3). Thus these data indicate that the underlying sensitivity of KO MEFs to IR may be in part via an impaired ability to control IR-induced oxidative stress.
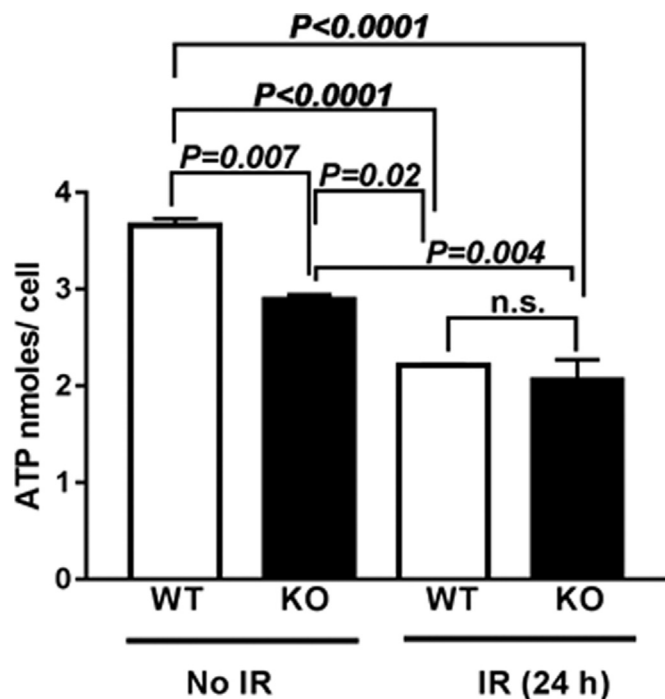
Fig. 5. *Cebpd*-KO MEFs showed significant reduction in ATP levels at 24 h post-irradiation. WT and KO MEFs were harvested at 0 and 24h post-irradiation (2 Gy) and whole cell extracts were prepared and analyzed for ATP levels. The data is plotted as an average of three biological replicates ± S.E.M.

3.4. Cebpd-KO MEFs show mitochondrial dysfunction after exposure to IR

Several studies have demonstrated that the exposure of cells to IR adversely affects the mitochondrial electron transport chain and respiration [21,53]. The cellular bioenergetics and cellular respiration in unirradiated versus irradiated WT and KO MEFs were measured using the Sea-horse XF flux analyzer (Fig. 4A). There were no significant differences between the WT and KO MEFs in their basal, ATP-linked, maximal, reserved respiratory capacity, non-mitochondrial respiration and proton leakage. However, at 24 h post-irradiation, KO MEFs showed significant reductions in basal respiration (0.63-fold), ATP-linked respiration (0.6-fold), maximal respiration (0.66-fold), reserved respiratory capacity (0.69-fold), proton leakage (0.76-fold) and non-mitochondrial respiration (0.67-fold) compared to respective WT MEFs (Fig. 4B-G). These results suggest that the mitochondria in the KO MEFs display severe dysfunction and are unable to cope up with the IR-induced oxidative stress.

3.5. Cebpd-KO MEFs express significantly reduced ATP levels after IR exposure

It is well known that mitochondrial dysfunction and IR-induced oxidative stress leads to reduction in ATP synthesis due to disruption of the proton gradient across the mitochondrial membrane [20]. We next investigated whether the mitochondrial dysfunction led to alterations in ATP production. KO MEFs showed a 0.8-fold decrease in ATP levels under basal conditions which showed a further 0.56-fold decrease at 24 h post-2 Gy exposure compared to unirradiated WT MEFs (Fig. 5). The reduced ATP levels could arise due to oxidation of the coenzymes NADH/NADPH of the mitochondrial electron transport chain.

We therefore examined whether there was increased oxidation of the coenzymes NADH/ NADPH. Contrary to our expectation, we found no significant differences in the levels of oxidized to reduced forms of the coenzymes NADH and NADPH between both the genotypes (Supplementary Fig. 1).

3.6. Cebpd-deficient MEFs expressed low levels of GSH, Cysteine and Methionine

Although we saw that ATP levels were significantly reduced in KO MEFs post-2 Gy exposure, we did not find any significant changes in the oxidation of the coenzymes NADH/NADPH of the mitochondrial electron transport chain. We next investigated whether the expression of the cellular antioxidant GSH, which is known to protect against radiation-induced oxidative damage [28] is impaired in the KO MEFs.

Interestingly, we found that KO MEFs expressed significantly lower levels of reduced GSH and GSSG compared to WT MEFs in irradiated as well as unirradiated conditions (Fig. 6A-B), which correlated with the increased ROS levels as shown by MitoSOX oxidation (Fig. 2). While the total GSH levels and GSH/GSSG were lower in KO MEFs, than WT MEFs (supplementary Fig. 2A, B). The decreased levels of GSH further correlated with reduced levels of its precursor amino acid-cysteine as well as methionine (Fig. 6C-D). Particularly the essential amino acid methionine is a precursor for cysteine, a rate limiting amino acid for GSH synthesis.

3.7. Cebpd-deficient MEFs accumulate high levels of 4-HNE protein adducts

It is known that increased oxidative stress results in increased chemical modifications of cellular proteins namely protein carbonylations and formation of 4-HNE adducts [54]. GSH plays a critical role in detoxification of 4-HNE and thus protects the cellular components from oxidative damage. Therefore, the expression of HNE-protein adduct formation as a marker of oxidative damage to the cellular proteins was examined in KO and WT MEFs at various timepoints post-irradiation. WT and KO MEFs express similar HNE-protein adduct formation under basal conditions, which was significantly elevated in KO MEFs after irradiation as compared to respective WT MEFs (Fig. 7). These results demonstrate an impaired ability to modulate endogenous ROS levels in irradiated cells leading to increased oxidative damage of the cellular proteins in KO MEFs.

3.8. Post-radiation survival of Cebpd-KO MEFs was rescued by pre-treatment with NAC and inhibited by BSO

To determine whether decreased GSH was the underlying cause of decreased post-radiation survival and increased radio-sensitivity of KO MEFs, we assessed the effect of the GSH precursor- NAC on IR-induced cell death. We found that treatment with NAC (5 mM) for 2 h prior to irradiation and 3 h post-irradiation did not have any significant effects on cell death measured by Annexin V staining in WT MEFs under basal condition or after exposure to 10 Gy (Fig. 8A). In contrast, unirradiated KO MEFs showed a 0.63-fold decrease when compared with respective WT MEFs. Compared to irradiated WT MEFs, irradiated KO MEFs showed a 0.43-fold decrease in cell death when treated with NAC which was significant (Fig. 8A).

Further we wanted to determine whether treatment of NAC led to improved clonogenic survival of WT and KO MEFs after exposure to IR. We found that treatment with NAC (5 mM) for 2 h prior to irradiation and 3 h post-irradiation showed a robust rescue of clonogenic survival of both irradiated WT and KO MEFs (Fig. 8B).

We also verified whether NAC treatment led to significant increase in GSH levels and was the underlying basis of increased clonogenic survival and decreased cell death in KO MEFs. NAC
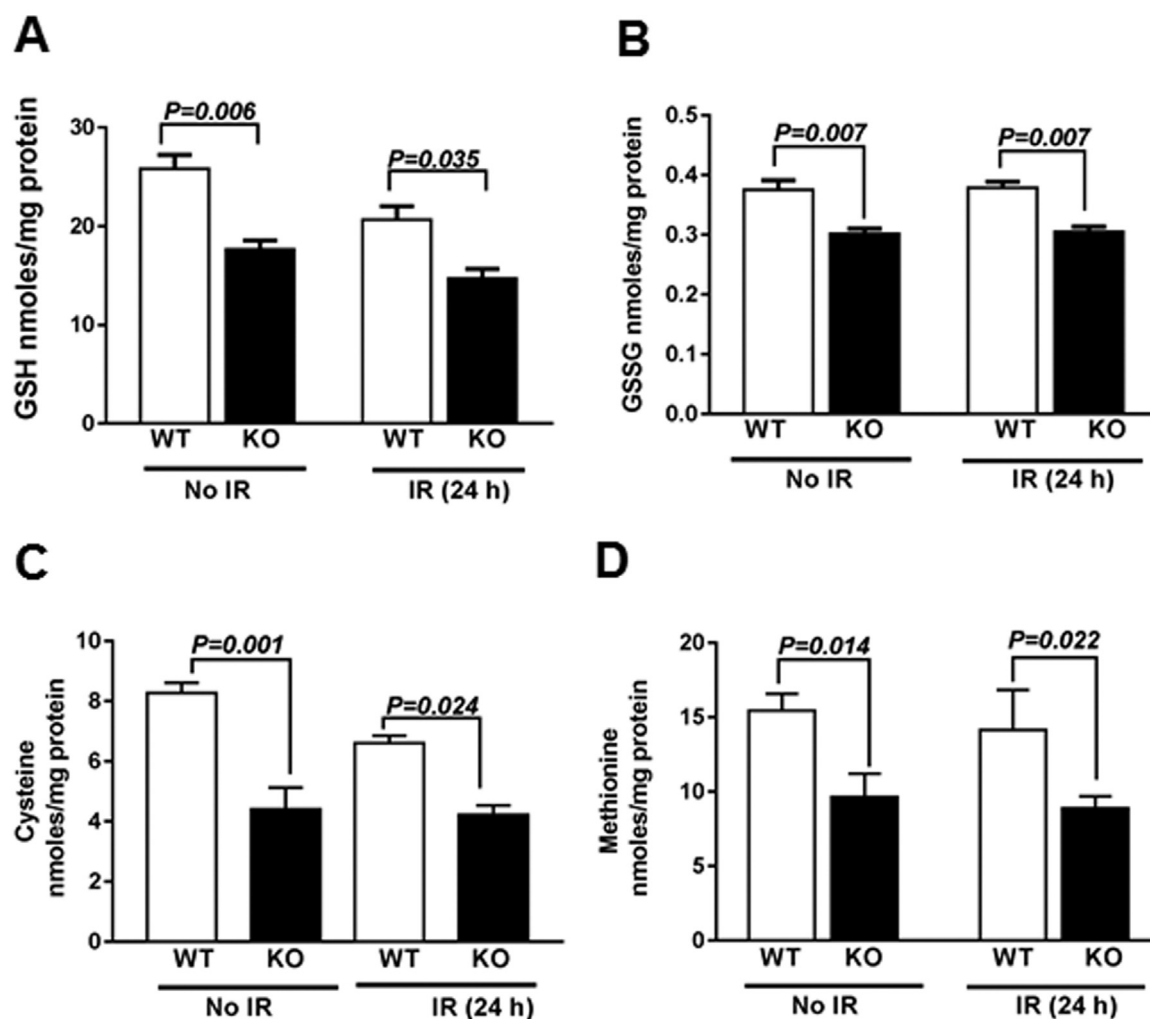
Fig. 6. *Cebpd*-KO MEFs show reduced expression of GSH and its precursor amino acid –cysteine as well as methionine. WT and KO MEFs were harvested at 0 and 24 h post-irradiation (2 Gy) and analyzed for the (A) GSH; (B) GSSG; (C) Cysteine and (D) Methionine and normalized to protein content. The data is plotted as an average of three biological replicates ± S.E.M.
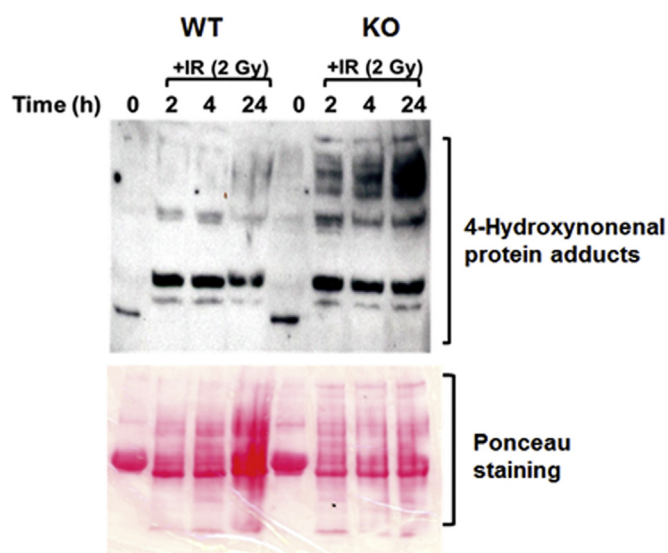
Fig. 7. *Cebpd*-KO MEFs display increased oxidative damage after IR exposure. WT and KO MEFs were harvested at 0, 2, 4 and 24 h post-IR (2 Gy) and probed with an antibody specific for 4-HNE. This is a representative blot showing the increased 4-HNE–protein adduct formation in KO MEFs at various timepoints post-irradiation. Ponceau S staining of the blot serves as a loading control.

treatment led to 1.35-fold increase in WT MEFs and 1.46-fold increase in GSH levels in the KO MEFs compared to respective irradiated WT and KO MEFs (Fig. 8C).

To further confirm the role of reduced GSH levels in the increased sensitivity of KO MEFS to IR exposure, we examined the effect of inhibition of the gamma-glutamate cysteine ligase, the rate limiting step of GSH biosynthesis by BSO on clonogenic survival of irradiated and unirradiated WT and KO MEFs. Here, pre-treatment with BSO stimulated the survival of unirradiated WT MEFs by 1.3-fold compared to KO MEFs (Fig. 8D). In the irradiated groups, BSO pre-treatment further decreased the survival of KO MEFs by 1.6-fold compared to that of WT MEFs and by 1.9-fold compared to that of KO MEFs. These data demonstrate that the underlying sensitivity of KO MEFs to IR is in part via the reduced GSH levels.

4. Discussion

In this study we describe a novel role for C/EBPδ in regulating IR-induced oxidative stress and induced mitochondrial dysfunction and thereby promoting post-radiation survival. The major findings of this study are that a loss of C/EBPδ results in increased basal as well as IR-induced ROS levels and mitochondrial dysfunction which led to increased apoptosis. Further we showed that
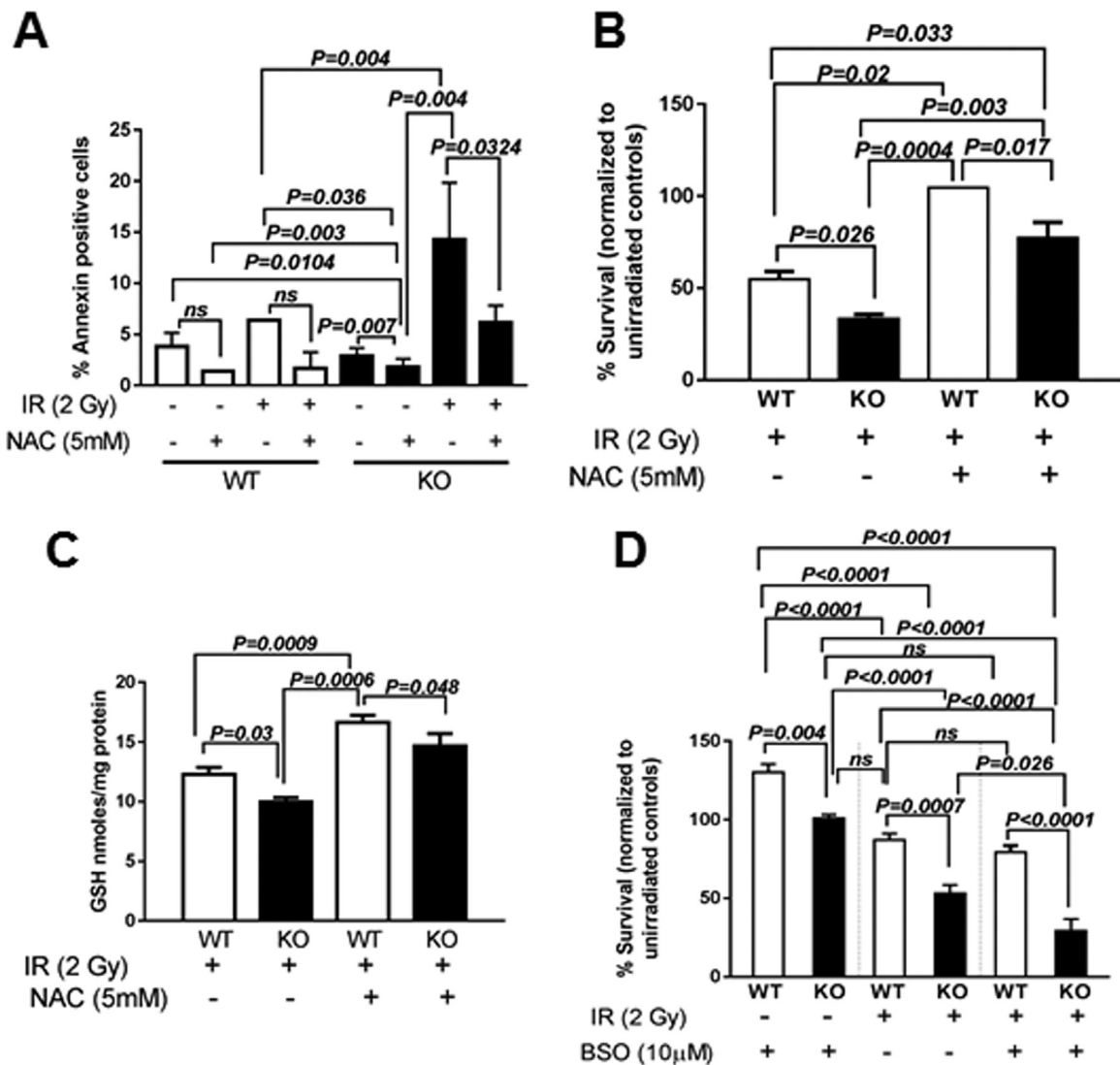
Fig. 8. The GSH-precursor NAC rescues post-radiation survival but the GSH inhibitor-BSO reduces survival of *Cebpd*-KO MEFs. WT and KO MEFs were treated with NAC (5 mM) for 2 h prior to IR exposure (10 Gy) and analyzed at indicated timepoints for (A) apoptosis using FITC Annexin V; (B) WT and KO MEFs were treated with NAC (5 mM) for 2 h prior to irradiation at 2 Gy and re-seeded for clonogenic assay 3 h post-irradiation and (C) cells were also harvested for GSH measurements; (D) KO and WT MEFs were treated with BSO (10 μM) for 24 h prior to irradiation at 2 Gy and re-seeded for clonogenic assay 3 h post-irradiation. The data for A and C are plotted as an average of 2–3 dishes ± S.E.M. The data for B and D are plotted as an average of 6 dishes each for the 2 biological replicates ± S.E.M.

C/EBPδ-deficiency led to decreased levels of GSH and its precursor amino acid-cysteine and its precursor-methionine. Thus our studies point to a novel role of C/EBPδ in redox regulation via modulation of GSH levels.

C/EBPδ is a transcription factor that has been implicated in the regulation of gene targets involved in inflammation, DNA damage response and oxidative stress, processes that also play a critical role in response of cells or tissues to IR exposure [32,36,39–42]. Survival of cells in response to IR exposure is dependent upon their ability to recover from IR-induced oxidative stress, DNA damage and inflammation [32,36,39–42]. A previous study has shown a role for C/EBPδ in detoxification of cisplatin-induced ROS levels by transcriptional upregulation of SOD1 [39]. Cells that overexpress SOD1 are known to be protected from IR-induced apoptosis [55–57]. It is possible that *Cebpd*-WT MEFs may upregulate antioxidant response genes which are perhaps impaired in the KO MEFs, thereby making them more susceptible to IR-induced cell death. Similar to the anti-apoptotic role of CEBPδ described in mammary epithelial cells and pancreatic beta cells [58,59], we found that *Cebpd*-WT MEFs protected from IR-induced apoptosis and promoted clonogenic survival compared to KO MEFs

(Fig. 1), which correlated with decreased ROS levels (Fig. 2).

The clonogenic survival of WT and KO MEFs upon pre-treatment with PEG-CAT prior to irradiation did not show significant change compared to the respective PEG-alone group, suggesting that the increased IR-induced cell death may be due to the increased $O_2^{\bullet-}$ levels. In contrast, PEG-SOD pre-treatment led to a further decrease in post-radiation clonogenic survival of both WT and KO MEFs compared to PEG-alone group. These results suggest that the cells accumulate increased H_2O_2 due to dismutation of IR-induced increased $O_2^{\bullet-}$ levels and points to a contributory role of IR-induced mitochondrial superoxide in promoting cell death. KO MEFs as well as WT MEFs showed a partial rescue of clonogenic survival, when treated with a combination of PEG-SOD+CAT, rather than individual treatment of PEG-SOD or PEG-CAT alone (Fig. 3). Overall these results suggest that both $O_2^{\bullet-}$ and H_2O_2 may contribute to the decrease in post-radiation survival in *Cebpd*-KO MEFs.

We also further investigated whether the increased ROS levels led to alterations of mitochondrial function in KO MEFs in response to IR. Although unirradiated KO MEFs show elevated ROS levels as shown by MitoSOX oxidation, there were no significant
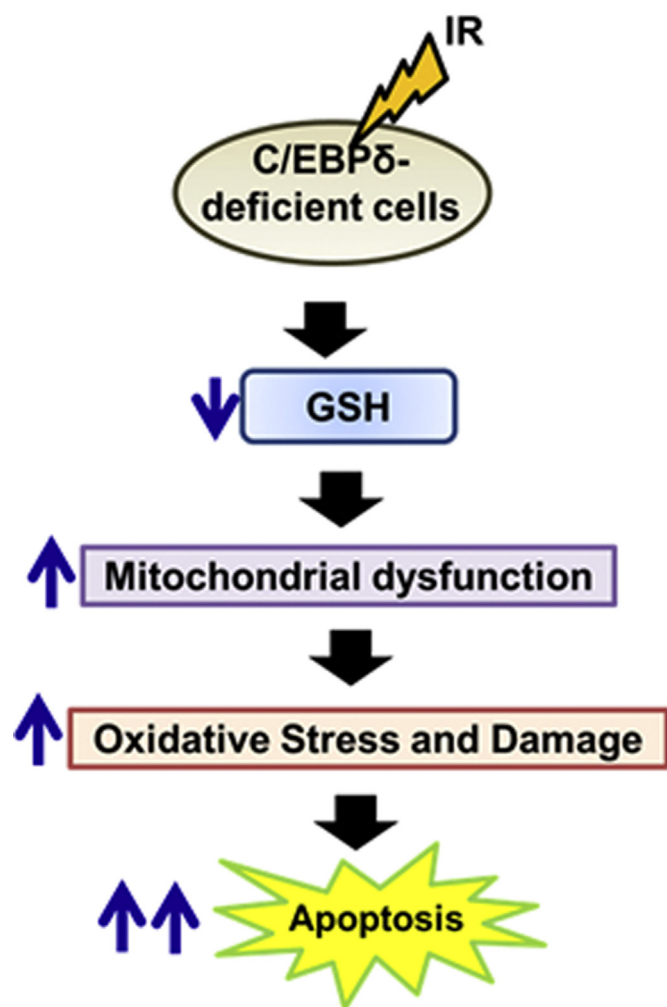
Fig. 9. Schematic model depicting the increased oxidative stress, mitochondrial dysfunction and reduced GSH levels that lead to IR-induced apoptosis of C/EBPδ-deficient cells.

differences in the mitochondrial function compared to that of WT MEFs as measured by OCR (Fig. 4A-B). This could be due to the robust induction of antioxidant genes under basal conditions in the KO MEFs but not after exposure to IR (*data not shown*). However post-irradiation, KO MEFs showed significant decreases in basal, ATP-dependent, maximal and reserved respiratory capacity as well as a decrease in proton leakage, indicative of mitochondrial dysfunction compared to WT MEFs (Fig. 4) which correlated with reduced ATP levels (Fig. 5). The decrease in reserved respiratory capacity of KO MEFs points to a deficiency in energy demanding bioenergetics response against IR-induced stress as described for *Sirt3*-knockdown cells [60].

In contrast WT MEFs showed an increase in the basal, ATP-dependent, maximal, reserved respiratory capacity and non-mitochondrial respiration, which is indicative of an adaptive response to IR-induced oxidative stress. The increased ROS levels in KO MEFs however did not show any impairment in the NAD^+/NADH and $NADP^+$/NADPH ratios, both under irradiated and unirradiated conditions, which led us to investigate the role of the cellular antioxidant GSH (Supplementary Fig. 1).

GSH plays a key role in maintaining the redox state that is critical for cellular activities [28,29]. It is known that the cellular antioxidant GSH protects against radiation-induced oxidative damage and the oxidation of GSH is an indicator of oxidative stress. Increased levels of GSH are known to suppress apoptosis [25,28]. We found that the KO MEFs express reduced levels of GSH compared to WT MEFs (Fig. 6A-B). In addition to reduced GSH levels, we also found that KO MEFs expressed reduced cysteine and methionine content (Fig. 6C-D).

Apart from its role in maintaining redox state of the cells, GSH is also involved in detoxification of ROS/RNS by direct interactions with enzymes like GSH-peroxidase and GSH-S-transferase [25,27]. 4-HNE is a lipid peroxidation-derived product, highly associated with the generation of ROS, hence used as a marker of oxidative stress [54]. 4-HNE is rapidly removed from the cells by phase II pathway using glutathione-S-transferases which use GSH as one of the substrates leading to its short half-life. We investigated whether the reduced GSH levels led to increased oxidative damage in the irradiated KO MEFs. The increased accumulation of 4-HNE protein adducts in the irradiated KO MEFs could be due to decreased clearing of 4-HNE protein adducts and correlates with the reduced GSH levels (Fig. 7). These studies suggest that reduced GSH levels contribute to the increased oxidative stress and increased sensitivity of KO MEFs post-IR exposure.

To further confirm the role of reduced GSH in promoting IR-induced cell death, we investigated the effects of the GSH precursor-NAC on IR-induced cell death of WT and KO MEFs. Although unirradiated and irradiated WT MEFs did not show significant reductions in apoptosis with NAC treatment, they showed a significant increase in GSH levels and rescue of clonogenic survival (Fig. 8A-C). These results suggest that GSH-independent pathways may also play a role in the post-radiation survival of WT MEFs.

In contrast, KO MEFs showed significant reductions in cell death in both unirradiated and irradiated groups, and significant increases in GSH levels compared to respective radiation alone treatment groups which explain the robust rescue of clonogenic survival (Fig. 8A-C). These results confirm the reduced GSH levels as one of the major players in the increased radiosensitivity of *Cebpd*-KO MEFs.

As expected we found that upon inhibiting GSH biosynthesis by BSO treatment for 24 h prior to irradiation, KO MEFs were further sensitized to IR and showed a decline in clonogenic survival compared to irradiated WT MEFs (Fig. 8D). While unirradiated WT and KO MEFS did not show any effect of BSO treatment, post-irradiation there was a significant decrease in post-radiation survival of BSO treated KO MEFs compared to radiation alone, but not in respective WT MEFs groups.

We speculate that *Cebpd*-KO MEFs may have defects in either GSH biosynthesis pathways or the GSH regeneration pathways similar to the Nrf2-/- MEFs [61]. This phenotype needs further investigation. Studies are currently underway utilizing a proteomics approach to identify the C/EBPδ-targets that may be downregulated in KO MEFs, leading to increased radiosensitivity. Overall, this study demonstrates a novel role of C/EBPδ in modulating oxidative stress via regulating the mitochondrial functions and maintaining the cellular levels of GSH (Fig. 9). Further studies are needed to investigate whether C/EBPδ may regulate genes involved in mitochondrial biogenesis and GSH metabolism.

Author contributions

SB, SAP, SKS, NAB, KJK and SBM: designed, performed experiments; SB, SAP, NAB and MHJ: analyzed results and wrote the paper.

Conflict of interest

None.

Acknowledgments

Appendix A. Supplementary material

Supplementary data associated with this article can be found in the online version at http://dx.doi.org/10.1016/j.freeradbiomed.2016.08.022.

References

[1] Hall E. J. a. G., A.J., Radiobiology for the Radiologist,. 6th edn, 2006.
[2] C.N. Andreassen, J. Isner, Genetic variants and normal tissue toxicity after radiotherapy: a systematic review, Radiat. Oncol. 92 (2009) 299–309.
[3] P. Prasanna, H. Stone, R. Wong, J. Capala, V., B, C. Coleman, Normal tissue protection for improving radiotherapy: where are the Gaps? Transl. Cancer Res 1 (2012) 35–48.
[4] M.E. Robbins, W. Zhao, Chronic oxidative stress and radiation-induced late normal tissue injury: a review, Int. J. Radiat. Biol. 80 (2004) 251–259.
[5] W. Zhao, D.I. Diz, M.E. Robbins, Oxidative damage pathways in relation to normal tissue injury, Br. J. Radiol. 80 (2007) S23–S31.
[6] S.W. Ryter, H.P. Kim, A. Hoetzel, J.W. Park, K. Nakahira, X. Wang, A.M. Choi, Mechanisms of cell death in oxidative stress, Antioxid. Redox Signal. 9 (2007) 49–89.
[7] D.R. Spitz, M. Hauer-Jensen, Ionizing radiation-induced responses: where free radical chemistry meets redox biology and medicine, Antioxid. Redox Signal. 20 (2014) 1407–1409.
[8] P. Okunieff, S. Swarts, P. Keng, W. Sun, W. Wang, J. Kim, S. Yang, H. Zhang, C. Liu, J.P. Williams, A.K. Huser, L. Zhang, Antioxidants reduce consequences of radiation exposure, Adv. Exp. Med. Biol. 614 (2008) 165–178.
[9] W.L. Santivasi, F. Xia, Ionizing radiation-induced DNA damage, response, and repair, Antioxid. Redox Signal. 21 (2014) 251–259.
[10] E.I. Azzam, J.P. Jay-Gerin, D. Pain, Ionizing radiation-induced metabolic oxidative stress and prolonged cell injury, Cancer Lett. 327 (2012) 48–60.
[11] R.,L. Auten, J.,M. Davis, Oxygen toxicity and reactive oxygen species: the devil is in the details, Pediatr. Res. 66 (2009) 121–127.
[12] J. Sun, Y. Chen, M. Li, Z. Ge, Role of antioxidant enzymes on ionizing radiation resistance, Free Radic. Biol. Med. 24 (1998) 586–593.
[13] G. Leonarduzzi, B. Sottero, G. Poli, Targeting tissue oxidative damage by means of cell signaling modulators: the antioxidant concept revisited, Pharmacol. Ther. 128 (2010) 336–374.
[14] D. Spitz, E. Azzam, J. Jian Li, D. Gius, Metabolic oxidation/reduction reactions and cellular responses to ionizing radiation: a unifying concept in stress response biology, Cancer and Metastasis Reviews, Kluwer Academic Publishers, Dordrecht, The Netherlands, 2004.
[15] D.R. Green, J.C. Reed, Mitochondria and apoptosis, Science 281 (1998) 1309–1312.
[16] J.F. Turrens, Mitochondrial formation of reactive oxygen species, J. Physiol. 552 (2003) 335–344.
[17] H.U. Simon, A. Haj-Yehia, F. Levi-Schaffer, Role of reactive oxygen species (ROS) in apoptosis induction, Apoptosis 5 (2000) 415–418.
[18] S. Kobashigawa, G. Kashino, K. Suzuki, S. Yamashita, H. Mori, Ionizing radiation-induced cell death is partly caused by increase of mitochondrial reactive oxygen species in normal human fibroblast cells, Radiat. Res. 183 (2015) 455–464.
[19] C.H. Wang, S.B. Wu, Y.T. Wu, Y.H. Wei, Oxidative stress response elicited by mitochondrial dysfunction: implication in the pathophysiology of aging, Exp. Biol. Med. 238 (2013) 450–460.
[20] J.J. Hwang, G.L. Lin, S.C. Sheu, F.J. Lin, Effect of ionizing radiation on liver mitochondrial respiratory functions in mice, Chin. Med. J. 112 (1999) 340–344.
[21] D. Dayal, S.M. Martin, K.M. Owens, N. Aykin-Burns, Y. Zhu, A. Boominathan, D. Pain, C.L. Limoli, P.C. Goswami, F.E. Domann, D.R. Spitz, Mitochondrial complex II dysfunction can contribute significantly to genomic instability after exposure to ionizing radiation, Radiat. Res. 172 (2009) 737–745.
[22] R. Kulkarni, B. Marples, M. Balasubramaniam, R.A. Thomas, J.D. Tucker, Mitochondrial gene expression changes in normal and mitochondrial mutant cells after exposure to ionizing radiation, Radiat. Res. 173 (2010) 635–644.
[23] Y.T. Yeung, K.L. McDonald, T. Grewal, L. Munoz, Interleukins in glioblastoma pathophysiology: implications for therapy, Br. J. Pharmacol. 168 (2013) 591–606 [Review].
[24] D.A. Dickinson, H.J. Forman, Glutathione in defense and signaling: lessons from a small thiol, Ann. N. Y. Acad. Sci. 973 (2002) 488–504.
[25] D.A. Dickinson, H.J. Forman, Cellular glutathione and thiols metabolism, Biochem. Pharm. 64 (2002) 1019–1026.
[26] R. Franco, J.A. Cidlowski, Apoptosis and glutathione: beyond an antioxidant, Cell Death Differ. 16 (2009) 1303–1314.
[27] V.I. Lushchak, Glutathione homeostasis and functions: potential targets for medical interventions, J. Amino Acids 2012 (2012) 26.
[28] A. Chatterjee, Reduced glutathione: a radioprotector or a modulator of DNA-repair activity? Nutrients 5 (2013) 525–542.
[29] Y.C. Awasthi, P. Chaudhary, R. Vatsyayan, A. Sharma, S. Awasthi, R. Sharma, Physiological and pharmacological significance of glutathione-conjugate transport, J. Toxicol. Environ. Health Part B Crit. Rev. 12 (2009) 540–551.
[30] R.V. Sekhar, S.G. Patel, A.P. Guthikonda, M. Reid, A. Balasubramanyam, G. E. Taffet, F. Jahoor, Deficient synthesis of glutathione underlies oxidative stress in aging and can be corrected by dietary cysteine and glycine supplementation, Am. J. Clin. Nutr. 94 (2011) 847–853.
[31] P. Diaz-Vivancos, A. de Simone, G. Kiddle, C.H. Foyer, Glutathione linking cell proliferation to oxidative stress, Free Radic. Biol. Med. 89 (2015) 1154–1164.
[32] D.P. Ramji, P. Foka, CCAAT/enhancer-binding proteins: structure, function and regulation, Biochem. J. 365 (2002) 561–575.
[33] X. Yu, J. Si, Y. Zhang, J. DeWille, CCAAT/Enhancer Binding Protein-delta (C/EBP-delta) regulates cell growth, migration and differentiation, Cancer Cell Int. 10 (2010) 48.
[34] J.P. O'Rourke, G.C. Newbound, J.A. Hutt, J. Dewille, CCAAT/enhancer-binding protein delta regulates mammary epithelial cell G0 growth arrest and apoptosis, J. Biol. Chem. 274 (1999) 16582–16589.
[35] A.M. Choi, S. Sylvester, L. Otterbein, N.J. Holbrook, Molecular responses to hyperoxia in vivo: relationship to increased tolerance in aged rats, Am. J. Respir. Cell Mol. Biol. (1995).
[36] A.M. Huang, C. Montagna, S. Sharan, Y. Ni, T. Ried, E. Sterneck, Loss of CCAAT/ enhancer binding protein delta promotes chromosomal instability, Oncogene 23 (2004) 1549–1557.
[37] T.R. Sarkar, S. Sharan, J. WANG, S.A. Pawar, C.A. Cantwell, P.F. Johnson, D. K. Morrison, J.M. Wang, E. Sterneck, Identification of a Src tyrosine kinase/ SIAH2 E3 ubiquitin ligase pathway that regulates C/EBPdelta expression and contributes to transformation of breast tumor cells, Mol. Cell Biol. 32 (2012) 320–332.
[38] V. Barbaro, A. Testa, I.E. Di, F. Mavilio, G. Pellegrini, L.M. De, C/EBPdelta regulates cell cycle and self-renewal of human limbal stem cells, J. Cell Biol. 177 (2007) 1037–1049.
[39] T.C. Hour, Y.L. Lai, C.I. Kuan, C.K. Chou, J.M. Wang, H.Y. Tu, H.T. Hu, C.S. Lin, W. J. Wu, Y.S. Pu, E. Sterneck, A.M. Huang, Transcriptional up-regulation of SOD1 by CEBPD: a potential target for cisplatin resistant human urothelial carcinoma cells, Biochem. Pharmacol. 80 (2010) 325–334.
[40] S.A. Pawar, T.R. Sarkar, K. Balamurugan, S. Sharan, J. WANG, Y. Zhang, S. F. Dowdy, A.M. Huang, E. Sterneck, C/EBP delta targets cyclin D1 for proteasome-mediated degradation via induction of CDC27/APC3 expression, Proc. Natl. Acad. Sci. USA 107 (2010) 9210–9215.
[41] J. Wang, T.R. Sarkar, M. Zhou, S. Sharan, D.A. Ritt, T.D. Veenstra, D.K. Morrison, A.M. Huang, E. Sterneck, CCAAT/enhancer binding protein delta (C/EBPdelta, CEBPD)-mediated nuclear import of FANCD2 by IPO4 augments cellular response to DNA Damage, Proc. Natl. Acad. Sci. USA 107 (2010) 16131–16136.
[42] K. Balamurugan, E. Sterneck, The many faces of C/EBPdelta and their relevance for inflammation and cancer, Int. J. Biol. Sci. 9 (2013) 917–933.
[43] S.A. Pawar, L. Shao, J. Chang, W. Wang, R. Pathak, X. Zhu, J. Wang, H. Hendrickson, M. Boerma, E. Sterneck, D. Zhou, M. Hauer-Jensen, C/EBP delta deficiency sensitizes mice to ionizing radiation-induced hematopoietic and intestinal injury, PLoS One 9 (2014) e94967.
[44] K.M. Robinson, M.S. Janes, J.S. Beckman, The selective detection of mitochondrial superoxide by live cell imaging, Nat. Protoc. 3 (2008) 941–947.
[45] J. Zielonka, B. Kalyanaraman, Hydroethidine- and MitoSOX-derived red fluorescence is not a reliable indicator of intracellular superoxide formation: another inconvenient truth, Free Radic. Biol. Med. 48 (2010) 983–1001.
[46] M.J. Borrelli, L.L. Thompson, W.C. Dewey, Evidence that the feeder effect in

mammalian cells is mediated by a diffusible substance, Int. J. Hyperth. 5 (1989) 99–103.

[47] A. Munshi, Marvette Hobbs, E. Meyn Raymond, Clonogenic cell survival assay, Methods Mol. Med. 110 (2005) 7.

[48] R. Pathak, S.A. Pawar, Q. Fu, P.K. Gupta, M. Berbee, S. Garg, V. Sridharan, W. Wang, P.G. Biju, K.J. Krager, M. Boerma, S.P. Ghosh, A.K. Cheema, H. P. Hendrickson, N. Aykin-Burns, M. Hauer-Jensen, Characterization of transgenic Gfrp knock-in mice: implications for tetrahydrobiopterin in modulation of normal tissue radiation responses, Antioxid. Redox Signal. 20 (2014) 1436–1446.

[49] M. Wu, A. Neilson, A.L. Swift, R. Moran, J. Tamagnine, D. Parslow, S. Armistead, K. Lemire, J. Orrell, J. Teich, S. Chomicz, D.A. Ferrick, Multiparameter metabolic analysis reveals a close link between attenuated mitochondrial bioenergetic function and enhanced glycolysis dependency in human tumor cells, Am. J. Physiol. Cell Physiol. 292 (2007) C125–C136.

[50] S. Banerjee, S.B. Melnyk, K.J. Krager, N. Aykin-Burns, L.G. Letzig, L.P. James, J. A. Hinson, The neuronal nitric oxide synthase inhibitor NANT blocks acet-aminophen toxicity and protein nitration in freshly isolated hepatocytes, Free Radic. Biol. Med. 89 (2015) 750–757.

[51] V. Stocchi, L. Cucchiarini, M. Magnani, L. Chiarantini, P. Palma, G. Crescentini, Simultaneous extraction and reverse-phase high-performance liquid chromatographic determination of adenine and pyridine nucleotides in human red blood cells, Anal. Biochem. 146 (1985) 118–124.

[52] S. Melnyk, M. Pogribna, I. Pogribny, R.J. Hine, S.J. James, A new HPLC method for the simultaneous determination of oxidized and reduced plasma ami-nothiols using coulometric electrochemical detection1, J. Nutr. Biochem. 10 (1999) 490–497.

[53] N. Aykin-Burns, B.G. Slane, A.T. Liu, K.M. Owens, M.S. O'Malley, B.J. Smith, F. E. Domann, D.R. Spitz, Sensitivity to low-dose/low-LET ionizing radiation in

mammalian cells harboring mutations in succinate dehydrogenase subunit C is governed by mitochondria-derived reactive oxygen species, Radiat. Res. 175 (2011) 150–158.

[54] H. Zhong, H. Yin, Role of lipid peroxidation derived 4-hydroxynonenal (4-HNE) in cancer: focusing on mitochondria, Redox Biol. 4 (2015) 193–199.

[55] Y. Peter, G. Rotman, J. Lotem, A. Elson, Y. Shiloh, Y. Groner, Elevated Cu/Zn-SOD exacerbates radiation sensitivity and hematopoietic abnormalities of Atm-deficient mice, EMBO J. 20 (2001) 1538–1546.

[56] G. Guo, Y. Yan-Sanders, B.D. Lyn-Cook, T. Wang, D. Tamae, J. Ogi, A. Khaletskiy, Z. Li, C. Weydert, J.A. Longmate, T.T. Huang, D.R. Spitz, L.W. Oberley, J.J. Li, Manganese superoxide dismutase-mediated gene expression in radiation-in-duced adaptive responses, Mol. Cell. Biol. 23 (2003) 2362–2378.

[57] A. Hosoki, S.I. Yonekura, Q.L. Zhao, L. WeiZ, I. Takasaki, Y. Tabuchi, L.L. Wang, S. Hasuike, T. Nomurat, A. Tachibana, K. Hashiguchi, S. Yonei, T. Kondo, Q. M. Zhang-Akiyama, Mitochondria-targeted Superoxide Dismutase (SOD2) regulates radiation resistance and radiation stress response in HeLa cells, J. Radiat. Res. 53 (2012) 58–71.

[58] J.A. Hutt, J.W. DeWille, Oncostatin M induces growth arrest of mammary epithelium via a CCAAT/enhancer-binding protein delta-dependent pathway, Mol. Cancer Ther. 1 (2002) 601–610.

[59] F. Moore, I. Santin, T.C. Nogueira, E.N. Gurzov, L. Marselli, P. Marchetti, D. L. Eizirik, The transcription factor C/EBP delta has anti-apoptotic and anti-inflammatory roles in pancreatic beta cells, PLoS One 7 (2012) e31062.

[60] J. Pfleger, M. He, M. Abdellatif, Mitochondrial complex II is a source of the reserve respiratory capacity that is regulated by metabolic sensors and pro-motes cell survival, Cell Death Dis. 6 (2015) e1835.

[61] C. Gorrini, I.S. Harris, T.W. Mak, Modulation of oxidative stress as an anticancer strategy, Nat. Rev. Drug Discov. 12 (2013) 931–947.